Saudi Pharmaceutical Journal 31 (2023) 101766

HOSTED BY

Contents lists available at ScienceDirect

Saudi Pharmaceutical Journal

journal homepage: www.sciencedirect.com

Original article

An integrated phytochemical, *in silico* and *in vivo* approach to identify the protective effect of *Caroxylon salicornicum* against cisplatin hepatotoxicity

Shaymaa A. Ramadan [a], Emadeldin M. Kamel [b], Reem S. Alruhaimi [c], Albandari Bin-Ammar [d], Madeha A. Ewais [a], Akef A. Khowailed [e], Emad H.M. Hassanein [f], Ayman M. Mahmoud [g,h,*]

[a] *Physiology Department, Faculty of Medicine, Beni-Suef University, Egypt*
[b] *Chemistry Department, Faculty of Science, Beni-Suef University, Egypt*
[c] *Department of Biology, College of Science, Princess Nourah bint Abdulrahman University, Riyadh, Saudi Arabia*
[d] *Department of Clinical Nutrition, College of Applied Medical Sciences, University of Hail, Saudi Arabia*
[e] *Physiology Department, Faculty of Medicine, Cairo University, Egypt*
[f] *Department of Pharmacology & Toxicology, Faculty of Pharmacy, Al-Azhar University-Assiut Branch, Egypt*
[g] *Department of Life Sciences, Faculty of Science and Engineering, Manchester Metropolitan University, Manchester, UK*
[h] *Physiology Division, Zoology Department, Faculty of Science, Beni-Suef University, Egypt*

ARTICLE INFO

Article history:
Received 24 June 2023
Accepted 27 August 2023
Available online 29 August 2023

Keywords:
Liver injury
Cisplatin
Caroxylon
Inflammation
Oxidative stress

ABSTRACT

Cisplatin (CIS) is a chemotherapeutic medication for the treatment of cancer. However, hepatotoxicity is among the adverse effects limiting its use. *Caroxylon salicornicum* is traditionally used for treating inflammatory diseases. In this investigation, three flavonoids, four coumarins, and three sterols were detected in the petroleum ether fraction of *C. salicornicum* (PEFCS). The isolated phytochemicals exhibited binding affinity toward Keap1, NF-κB, and SIRT1 *in silico*. The hepatoprotective role of PEFCS (100, 200 and 400 mg/kg) was investigated *in vivo*. Rats received PEFCS for 14 days and CIS on day 15. CIS increased ALT, AST and ALP and caused tissue injury along with increased ROS, MDA, and NO. Hepatic NF-κB p65, pro-inflammatory mediators, Bax and caspase-3 were increased in CIS-treated animals while antioxidants and Bcl-2 were decreased. PEFCS mitigated hepatocyte injury, and ameliorated transaminases, ALP, oxidative stress (OS) and inflammatory markers. PEFCS downregulated pro-apoptosis markers and boosted Bcl-2 and antioxidants. In addition, PEFCS upregulated Nrf2, HO-1, and SIRT1 in CIS-administered rats. In conclusion, PEFCS is rich in beneficial phytoconstituents and conferred protection against liver injury by attenuating OS and inflammation and upregulating Nrf2 and SIRT1.
© 2023 The Author(s). Published by Elsevier B.V. on behalf of King Saud University. This is an open access article under the CC BY-NC-ND license (http://creativecommons.org/licenses/by-nc-nd/4.0/).

1. Introduction

Drug-induced liver injury (DILI) is a pathological status caused by the intake of medicinal compounds and manifested as abnormalities in liver structure and function (Bleibel et al., 2007). Owing to its vital functions, including the detoxication and chemical modification of drugs and xenobiotics, the liver is prone to drug toxicity and the number of drugs causing DILI has been reported to exceed a thousand (Bernal and Wendon 2013). Hepatotoxicity is a common reason for drug withdrawal because the potential to provoke DILI is often realized upon use in clinical settings (Russmann et al., 2009). The risk factors of DILI include drug- and host-dependent factors and an increase in the incidence was associated with increasing age and impaired drug clearance (Moore et al., 2007). The generation of reactive metabolites during drug metabolism increases the production of excess reactive oxygen species (ROS), resulting in oxidative injury and apoptosis (Aithal 2015). The hepatocytes are equipped with antioxidants to counteract excess ROS; however, dysregulation of this defense system contributes to the development of DILI. In addition, inflammation promoted by the ROS or innate immune system is implicated in the progression and severity of DILI (Aithal 2015).

* Corresponding author at: Department of Life Sciences, Faculty of Science and Engineering, Manchester Metropolitan University, Manchester M1 5GD, UK.
E-mail address: a.mahmoud@mmu.ac.uk (A.M. Mahmoud).
Peer review under responsibility of King Saud University.

Production and hosting by Elsevier

https://doi.org/10.1016/j.jsps.2023.101766
1319-0164/© 2023 The Author(s). Published by Elsevier B.V. on behalf of King Saud University.
This is an open access article under the CC BY-NC-ND license (http://creativecommons.org/licenses/by-nc-nd/4.0/).

Cisplatin (CIS) is a potent metal-based chemotherapeutic agent widely used for treating many cancers (Ghosh 2019). Excessive generation of ROS and its ability to bind and block the replication of DNA and the production of mRNA and proteins are among the cytotoxic mechanism of CIS (Brozovic et al., 2010). CIS is effective against testicular, cervical, gastric and ovarian tumors; however, adverse effects, including DILI, and lung and kidney injuries limit its clinical use (Ghosh 2019). The role played by oxidative and inflammatory reactions in CIS hepatotoxicity pinpoints the importance of their attenuation as a treatment strategy.

The activation of the cytoprotective proteins nuclear factor erythroid 2–related factor 2 (Nrf2) and Sirtuin 1 (SIRT1) was effective in counteracting CIS toxicity (Sami et al., 2022). Nrf2 responds to increased ROS by dissociating from Keap1 to promote the transcription of heme oxygenase (HO)-1 and other antioxidants (Satta et al., 2017) and its activation was effective in attenuating oxidative injury and inflammation caused by chemotherapeutic agents, including CIS (Mahmoud et al., 2017a). SIRT1 is a histone deacetylase involved in numerous cellular processes (Haigis and Guarente 2006) and its activation can protect the cells and increase cell survival under stress conditions (Raynes et al., 2013). SIRT1 can inhibit inflammation and tissue injury by deacetylating many signaling molecules, including NF-κB (Chen et al., 2020). Its activation prevented CIS nephrotoxicity (Chen et al., 2020), and different liver disorders, such as steatosis, fibrosis, hepatocarcinogenesis, and hepatotoxicity (reviewed in (Sayed et al., 2020)).

Caroxylon salicornicum (C. salicornicum) is a plant of the family *Chenopodiaceae* and found in many countries, including Egypt (Boulos 2005). It is a desert shrub distributed in many countries and used in folk medicine for treating diabetes, sepsis, ulcer, tuberculosis, and inflammatory disorders (Ajabnoor et al., 1984, Bibi et al., 2010). This study aimed to define the phytoconstituents

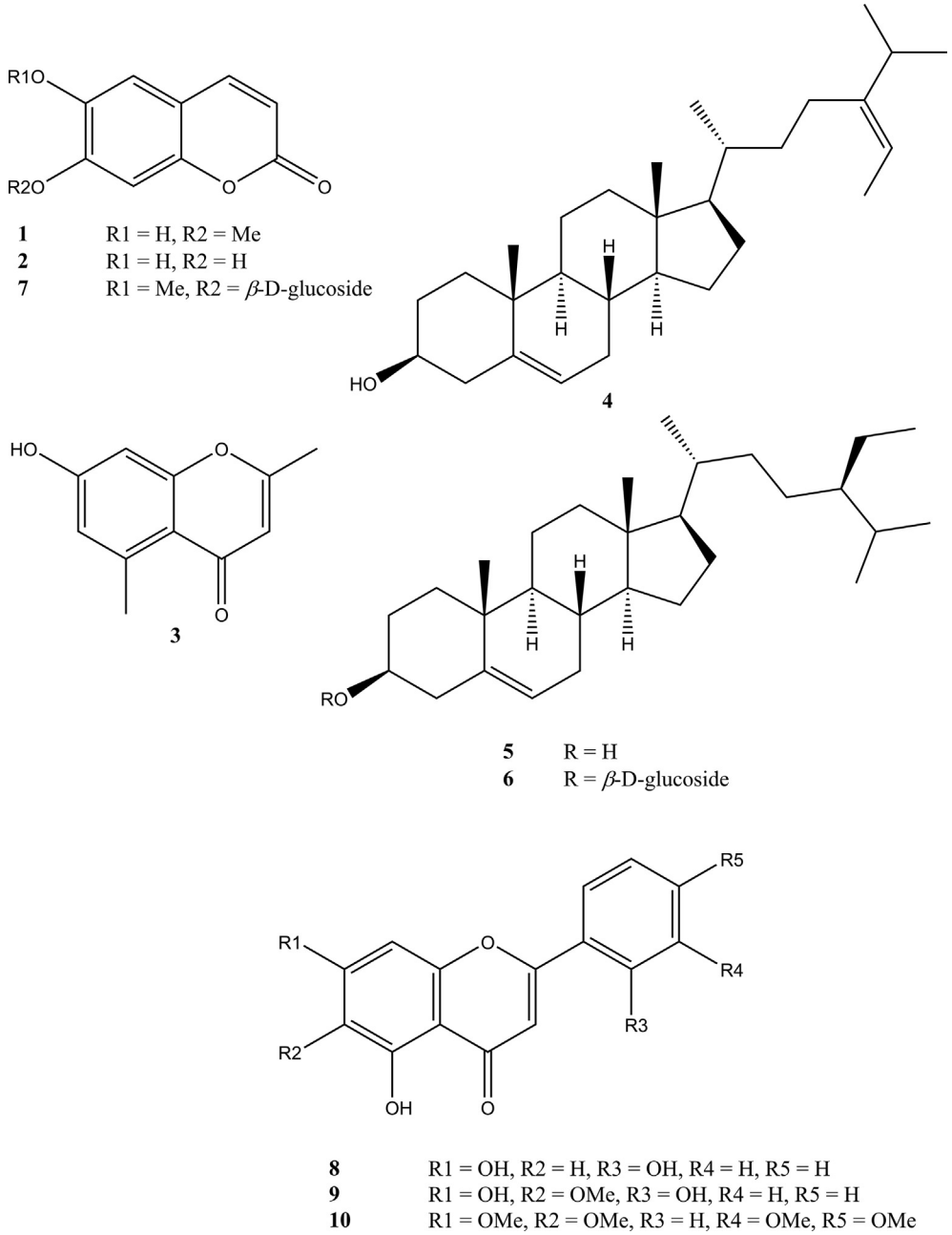

Fig. 1. Chemical structure of the compounds isolated from PEFCS.

and assess the effect of petroleum ether fraction of *C. salicornicum* ethanolic extract (PEFCS) on CIS hepatotoxicity, emphasizing oxidative and inflammatory responses, and Nrf2 and SIRT1 signaling.

2. Materials & methods

2.1. General

NMR spectral data of isolated compounds were determined on Bruker AM-500 spectrometer at 500 MHz for PNMR and 100 MHz for ^{13}C NMR. Optical rotation was detected with a Rudolph Autopol III polarimeter. UV spectra were measured from a Shimadzu UV–Vis 160i spectrophotometer. HREIMS and EIMS mass analyses were performed on Finnigan MAT TSQ 700 mass spectrometer. Shimadzu FTIR-8400 instrument was employed for IR spectral analysis on KBr pellets.

2.2. Plant collection, extraction, and isolation of phytoconstituents

The fresh plant was collected from a desert area close to the city of Beni-Suef and identified and authenticated by a taxonomist. The plant was dried, powdered and 3 kg was extracted by ethanol (EtOH) at room temperature (RT) and the solvent was removed *in vacuo* (Ahmad and Eram 2011). The residue (218 g) was dissolved in warm water and successively partitioned between petroleum ether (500 mL × 2), ethyl acetate (EA; 500 mL × 2), chloroform (500 mL × 2) and *n*-butanol (500 mL × 2). The organic phases were evaporated to afford the corresponding extracts (9.5 g, 8 g, 13 g and 29 g, respectively). The petroleum ether extract was chromatographed over silica gel column using hexane/EA as an eluent (100:0 to 0:100, *v*/*v*), to give 27 fractions which were combined into 14 fractions (F1-F14) following their TLC profile. Fractions with interesting compounds were considered for further purification steps. Fractions F3-F8 were combined and further applied to silica gel column and eluted with chloroform/methanol (MeOH) (70:30 to 0:100, *v*/*v*) to afford 35 sub fractions (E1-E35), subfractions E5-E18 were combined and purified over silica gel column eluted with *n*-hexane/EA (15:5) to produce compounds **4** (23 mg) and **5** (18 mg). Subfraction E23-E28 were also combined and applied to silica gel column with solvent system *n*-hexane/EA of increasing polarity. The fraction obtained with *n*-hexane/EA (13:7) produced compound **6** (19 mg). The EA fraction was run on silica gel column and gradient elution started with petroleum ether/acetone (50:5 to 10:5, *v*/*v*) to afford 13 fractions (C1-C13). Fractions C1, C3 and C5-C7 were combined, chromatographed over polyamide 6S followed by elution using MeOH/water (30:70 to 100:0, *v*/*v*), affording 20 subfractions (S1-S20). Subfractions S8-S18 were further purified over Sephadex LH-20 column using MeOH giving purified compounds **1** (15 mg), **2** (19 mg), and **3** (21 mg). The combined subfractions S19 and S20 were purified and eluted with MeOH to afford compound **7** (14 mg). Following fractionation of the *n*-butanolic soluble fraction, elution with toluene and then toluene/MeOH mixture gave 32 main fractions (combined into 11 fractions according to the TLC profile (A1-A11)). Factions 2 and 5–7 were combined, ran on a silica gel column and eluted with EA-MeOH-water (8.5:1:0.5) to afford 17 subfractions (B1-B17). The combined subfractions B5-B12 were chromatographed over Sephadex LH-20 and elution with MeOH afforded compounds **8** (16 mg) and **10** (20 mg), whereas the elution of B14-B16 dichloromethane/acetone (9.5:0.5) afforded compound **9** (18 mg).

2.3. Animals and treatments

Thirty-six male Wistar rats (170–180) g were included in this investigation. The rats were kept in standard cages (3 rats/cage) under standard temperature (23 ± 1 °C) and humidity (50–60%)

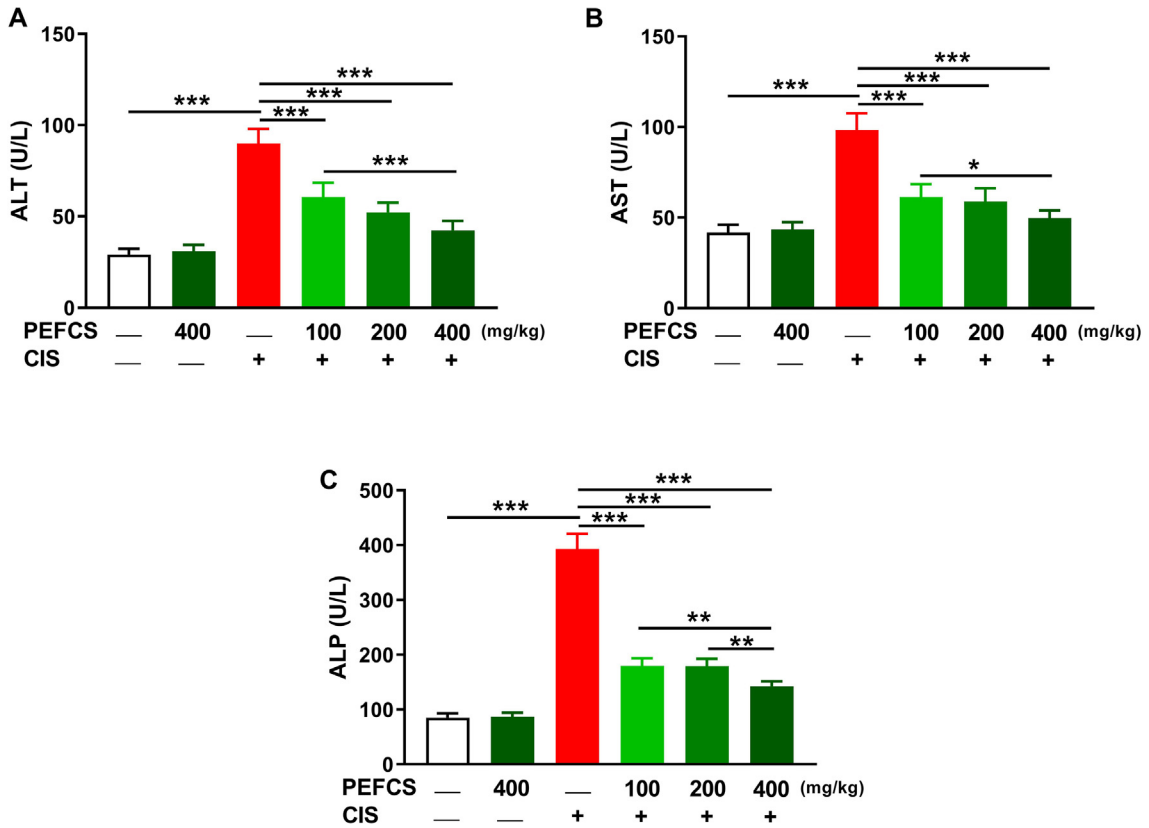

Fig. 2. PEFCS ameliorated serum ALT (A), AST (B) and ALP (C) in CIS-administered rats. Data are Mean ± SEM, (n = 6). *P < 0.05, **P < 0.01 and ***P < 0.001.

on a 12 h light/dark cycle. The rats were given free access to food and water and kept for two weeks before the onset of the experiment to exclude any intercurrent infection. The experiment was approved by the Ethics Committee of Beni-Suef University (Ethical approval no.: 020–96). The animals were divided into six groups (n = 6) as follows:

Group I: Control.

Group II: received 400 mg/kg PEFCS.

Group III: received an intraperitoneal (i.p.) injection of 7 mg/kg CIS (Sigma, USA) (Zhang et al., 2017) on day 15.

Group IV: received 100 mg/kg PEFCS.

Group V: received 200 mg/kg PEFCS.

Group VI: received 400 mg/kg PEFCS.

PEFCS was dissolved in 0.5% carboxymethyl cellulose (CMC) as a vehicle and orally administered for 14 days and CIS was injected i.p. on day 15. Groups IV, V, and VI received i.p. injection of 7 mg/kg CIS on day 15. Groups I and III received the vehicle orally for 14 days and Groups I and II received i.p. saline on day 15. 500 and 750 mg/kg doses of this plant extract showed protection against carbon tetrachloride (CCl_4) hepatotoxicity in rats (Ahmad and Eram 2011). The dose-dependent effect of PEFCS was evaluated in this study. Three days post CIS injection, blood was collected via cardiac puncture under ketamine (100 mg/kg, i.p.) anesthesia. The rats were euthanized with cervical dislocation, immediately dissected and samples from the liver were collected and fixed in 10% neutral-buffered formalin

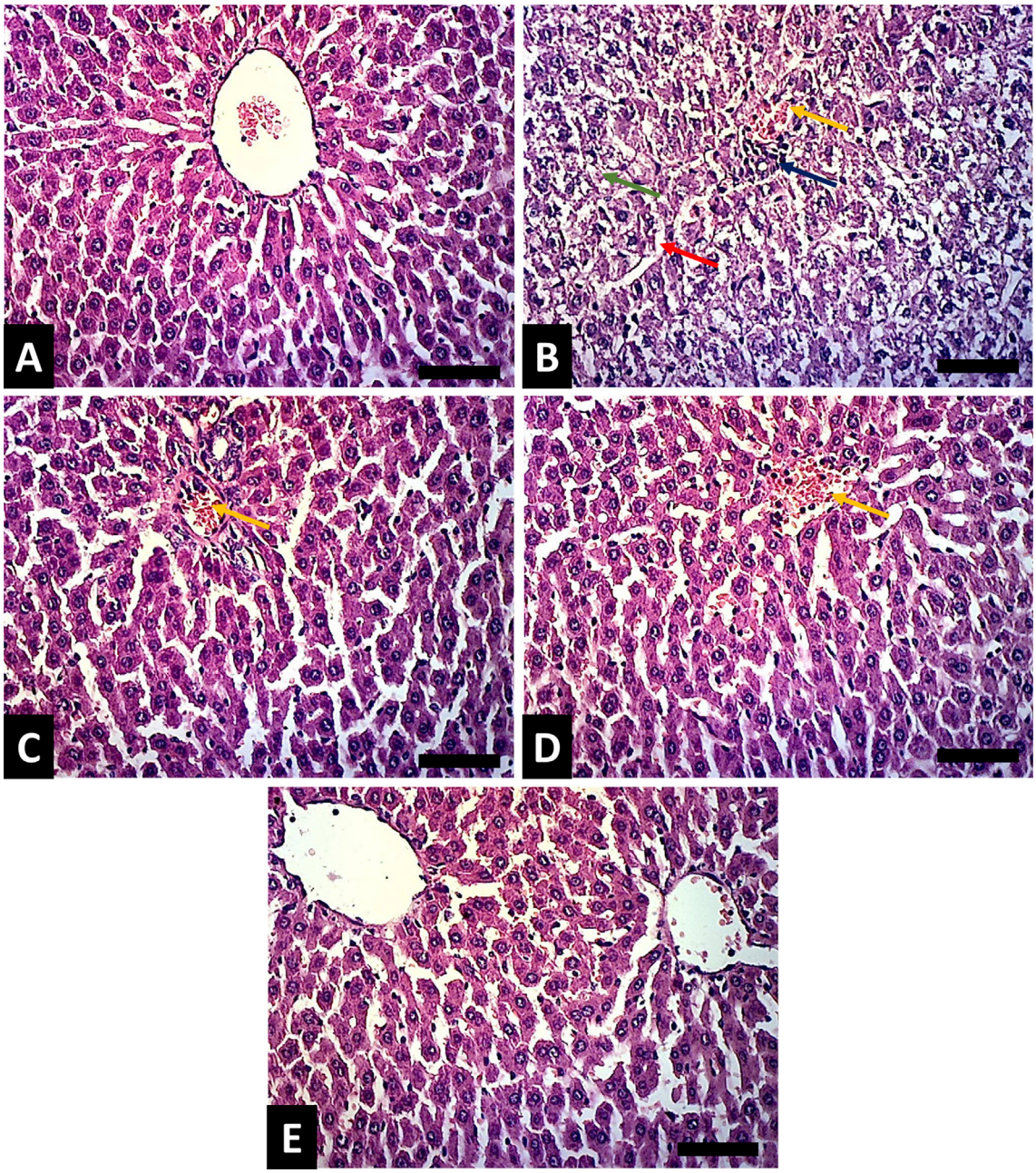

Fig. 3. PEFCS attenuated histopathological alterations in liver of CIS-administered rats. H&E-stained sections in the liver of (A) control rats showing normal central vein and well organized radially arranged hepatic cords, (B) CIS-induced rats showing disrupted organization of hepatic cords, congested blood vessels (yellow arrow), inflammatory cell infiltration (blue arrow), necrosis (green arrow), dilated sinusoids (red arrow), and vacuolar and hydropic degeneration in hepatocytes, (C-E) CIS-induced rats received 100 (C), 200 (D) and 400 mg/kg (E) PEFCS showing ameliorated liver injury and improved the histological architecture where only slight congestions (yellow arrow). (Scale bar = 50 μm).

(NBF) while others were homogenized in cold Tris-HCl buffer (pH = 7.4). The supernatant of the homogenate was separated by centrifugation. Additional liver samples were kept frozen in RNAlater (Thermofisher).

2.4. Biochemical investigations

The transaminases (ALT and AST) and ALP were determined using Spinreact (Spain) kits and TNF-α and IL-1β, NF-κB p65 and 8-Oxo-dG were assayed using ELISA. ROS were determined using H_2DCF-DA, and malondialdehyde (MDA) (Ohkawa et al., 1979), nitric oxide (NO) (Grisham et al., 1996), catalase (CAT) (Cohen et al., 1970), reduced glutathione (GSH) (Ellman 1959), HO-1 (Abraham et al., 1985), and superoxide dismutase (SOD) (Marklund and Marklund 1974) were assayed spectrophotometrically in the homogenized liver samples.

2.5. Histopathology and immunohistochemistry (IHC)

The fixed liver samples were processed for routine staining with hematoxylin and eosin (H&E) and blindly examined. Other sections were treated with 0.05 M citrate buffer (pH 6.8) to retrieve antigen. After treatment with 0.3% hydrogen peroxide (H_2O_2) and washing, the sections were probed overnight with antibodies for iNOS, caspase-3, and NF-kB p65 (Biospes, China) at 4 °C. After incubation with the 2^{ry} antibodies, color was developed using DAB in H_2O_2, Mayer's hematoxylin counterstaining was carried out. Intensity of the developed color was measured using ImageJ (NIH, USA).

2.6. qRT-PCR

The changes in the mRNA levels of Nrf2, SIRT1, Bax, miR-34A, and Bcl-2 were evaluated (Sami et al., 2022). Total RNA was isolated, quantified and samples with OD260/OD280 nm ≥ 1.8 were

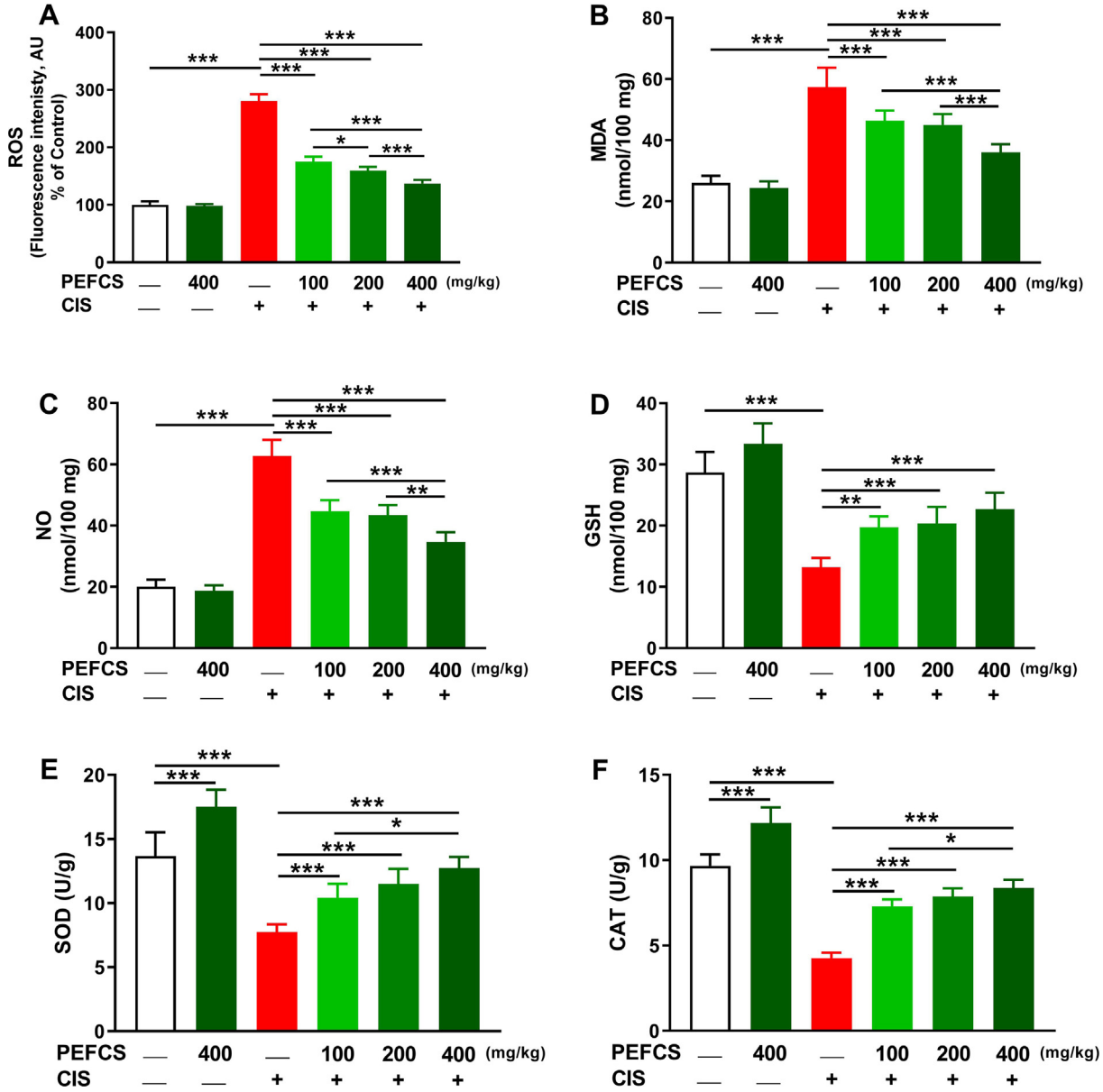

Fig. 4. PEFCS decreased hepatic ROS (A), MDA (B) and NO (C), and increased GSH (D), SOD (E) and CAT (F) in CIS-treated rats. Data are Mean ± SEM, (n = 6). *P < 0.05, **P < 0.01 and ***P < 0.001.

used for cDNA synthesis. The amplification of cDNA was carried out with SYBR Green MM and primers (Suppl. Table I). The results were calculated with $2^{-\Delta\Delta Ct}$ method (Livak and Schmittgen, 2001).

2.7. Molecular docking (MD)

The binding of PEFCS phytochemicals with Keap1 (PDB ID: 4L7B), SIRT1 (PDB ID: 4ZZJ) and NF-κB-DNA complex (PDB ID: 1LE9) was evaluated using AutoDock Vina and Autodock Tools (ADT) v1.5.6 as we recently reported (Sami et al., 2022).

2.8. Statistical analysis

The results are expressed as mean ± SEM. After testing the normality, one-way ANOVA and Tukey's post-hoc test were employed for multiple comparisons using GraphPad Prism 8. A $P < 0.05$ was considered significant.

3. Results

3.1. Phytochemical investigation

PEFCS afforded ten known compounds (**1**–**10**) (Fig. 1), corresponding to three flavonoids, four coumarins and three sterols. The isolated compounds were elucidated as isoscopoletin (**1**) (Bao et al., 2019), aesculetin (**2**) (Li et al., 2004), altechromone A (**3**) (Zhao et al., 2020), fucosterol (**4**) (Falsone et al., 1994), β-sitosterol (**5**) (Nes et al., 1992), β-sitosterol-3-O-β-D-glucoside (6) (Rehman et al., 2018), scopolin (**7**) (Tsukamoto et al., 1985), 5,7,2′-trihydroxyflavone (**8**) (Miyaichi et al., 2006), 5,7,2′-trihydroxy-6-methoxyflavone (**9**) (Agrawal 2013) and 5-hydroxy-6,7,3′,4′-tetramethoxyflavone (**10**) (Alwahsh et al., 2015).

3.2. PEFCS ameliorates liver function in CIS-administered rats

Circulating markers and histological examination were used for assessing the hepatoprotective effect of PEFCS in CIS-administered rats. ALT (Fig. 2A), AST (Fig. 2B) and ALP (Fig. 2C) were elevated significantly ($P < 0.001$) and treatment with PEFCS ameliorated their activities in CIS-administered rats. Normal rats that received 400 mg/kg PEFCS didn't show changes in serum transaminases and ALP.

The stained sections from the control rats (Fig. 3A) showed normal hepatocytes, sinusoids, and central vein whereas CIS caused vacuolar and hydropic degeneration in hepatocytes, congestion, necrosis and inflammatory cell infiltration (Fig. 3B). Treatment with 100 (Fig. 3C), 200 (Fig. 3D) and 400 mg/kg (Fig. 3E) PEFCS ameliorated CIS-induced hepatocyte injury and only slight congestion could be seen.

3.3. PEFCS prevents CIS-induced liver oxidative stress

ROS, MDA and NO were elevated in CIS-administered animals ($P < 0.001$) as illustrated in Fig. 4A, 4B, and 4C, respectively. CIS remarkably decreased hepatic GSH, SOD and CAT (Fig. 4D-F). All doses of PEFCS decreased ROS, MDA and NO and increased hepatic antioxidants in CIS-administered rats.

3.4. PEFCS prevents CIS-induced hepatic inflammation

NF-κB p65, iNOS, TNF-α and IL-1β were assessed to evaluate the anti-inflammatory effect of PEFCS. IHC (Fig. 5A,B) revealed upregulation of NF-κB p65 in CIS-administered rats ($P < 0.001$), findings that were supported by ELISA that showed a noticeable increase (Fig. 5C). iNOS (Fig. 6A,B), TNF-α (Fig. 6C) and IL-1β (Fig. 6D) were

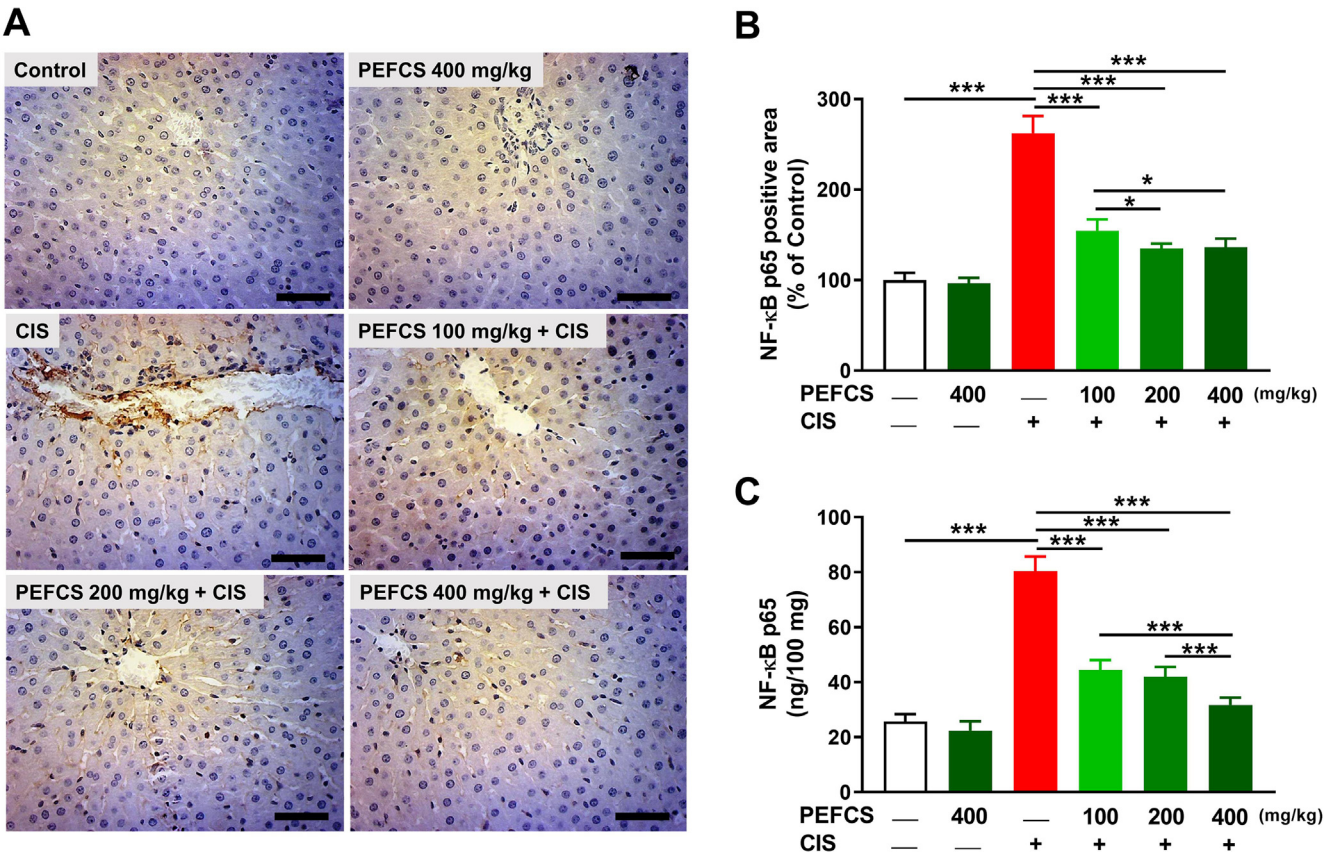

Fig. 5. PEFCS downregulated NF-κB p65 in the liver of CIS-treated rats. (A) Photomicrographs of NF-κB p65-immunostained sections in the liver of rats. (B) Image analysis showing changes in hepatic NF-κB p65 expression. (C) PEFCS decreased hepatic NF-κB p65 in CIS-administered rats. Data are Mean ± SEM, ($n = 6$). *P < 0.05 and ***P < 0.001.

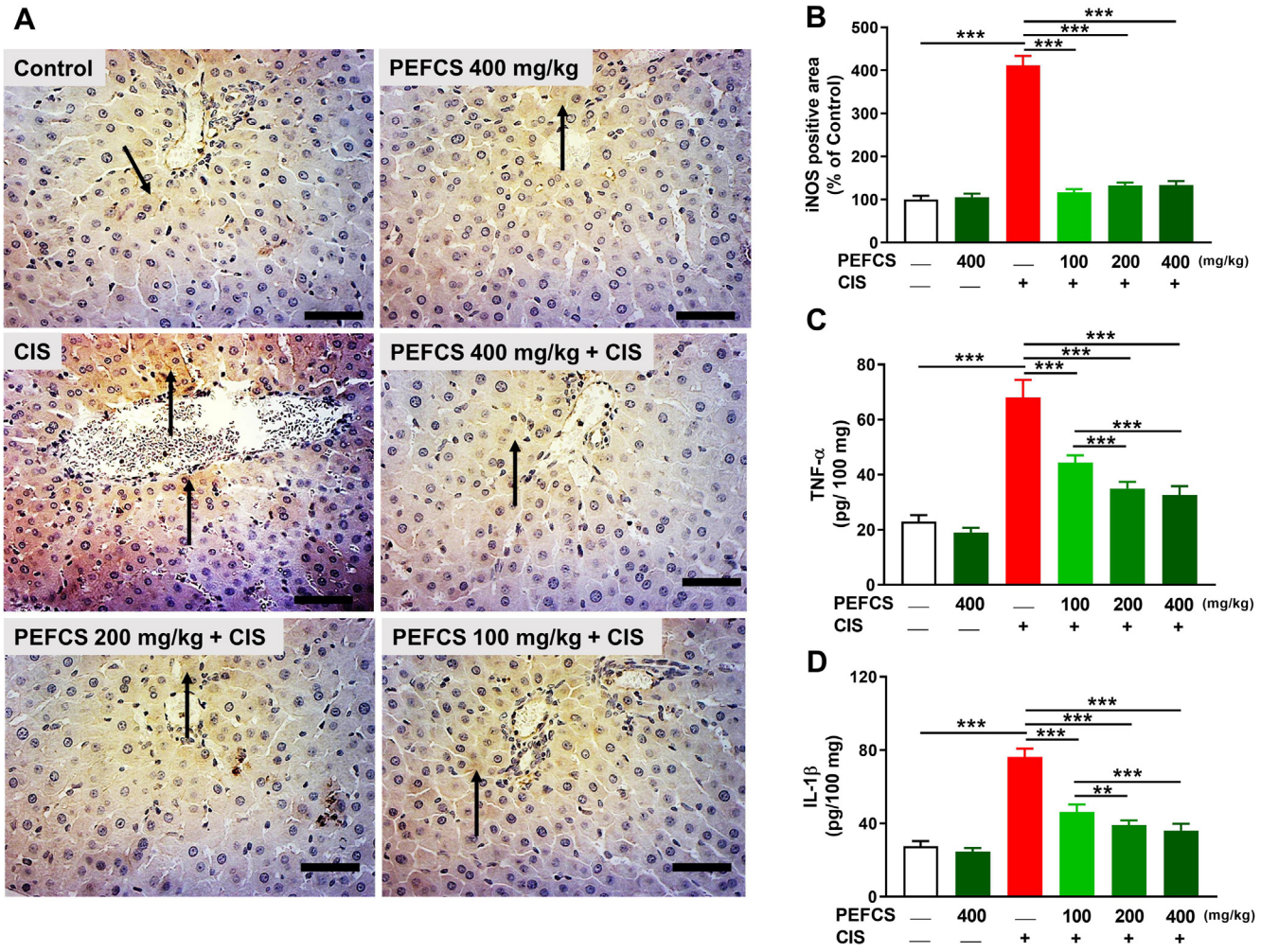

Fig. 6. PEFCS downregulated iNOS, TNF-α and IL-1β in the liver of CIS-administered rats. (A) Photomicrographs of iNOS-immunostained sections in the liver of rats. (B) Image analysis showing changes in hepatic iNOS expression. (C-D) PEFCS decreased hepatic TNF-α (C) and IL-1β (D) in CIS-administered rats. Data are Mean ± SEM, (n = 6). **P < 0.01 and ***P < 0.001.

upregulated in the liver of CIS-administered rats. Treatment with PEFCS remarkably decreased NF-κB p65, iNOS, TNF-α and IL-1β in CIS-treated animals.

As shown in Fig. 7, the isolated compounds showed affinity towards NF-κB with compounds **6**, **5**, **4** and **10** exhibited the lowest binding energy (-10.4, −10.1, −10 and −10 kcal/mole, respectively). Compound **6** forms polar interactions with Arg33, Asn186, Glu193 and Asp217 and hydrophobic interactions with Lys218, Arg246, Gln247, Lys272, Gln306 and Phe307. Compound **5** forms polar bonding with Arg246 and hydrophobic interactions with Lys218, Arg33, Arg187, Arg305 and Phe307 of NF-κB (Suppl. Table II).

3.5. PEFCS attenuates CIS-induced apoptosis and DNA damage

CIS downregulated BCL-2 mRNA (Fig. 8A) and increased BAX (Fig. 8B) and BAX/BCL-2 ratio (Fig. 8C) in the liver of rats (P < 0.001). A significant increase in caspase-3 (Fig. 8D-E) and 8-Oxo-dG (Fig. 8F) was observed in CIS-treated rats. PEFCS enhanced BCL-2 and dose dependently diminished BAX, caspase-3 and 8-Oxo-dG in rats challenged with CIS.

3.6. PEFCS modulates Nrf2/HO-1 and microRNA-34a/SIRT1 signaling in CIS-administered rats

Nrf2 mRNA (Fig. 9A) and HO-1 activity (Fig. 9B) were declined in the liver of CIS-treated rats (Fig. 9A) and treatment with PEFCS ameliorated these alterations where it upregulated Nrf2 mRNA and HO-1 activity. MD revealed the binding affinity of all compounds with Keap1(Fig. 9C,D and Suppl. Table III). Compounds **6**, **4** and **9** exhibited 10.0, 9.7 and 9.6 kcal binding energy, respectively.

CIS increased microRNA-34a and decreased SIRT1 as depicted in Fig. 10A and 10B, respectively. PEFCS prevented these alterations induced by CIS and MD revealed the binding affinity of its contained phytochemicals with SIRT1 (Fig. 10C,D and Suppl. Table IV).

4. Discussion

The present study explored the phytochemical constituents of PEFCS and assessed its protective effect on hepatotoxicity induced by CIS. Previously reported phytochemical screening of the genus *Haloxylon* detected flavonoids, alkaloids, coumarins, triglycerides and steroidal glycosides (Azizuddin and Mustafa, 2013). Here, the

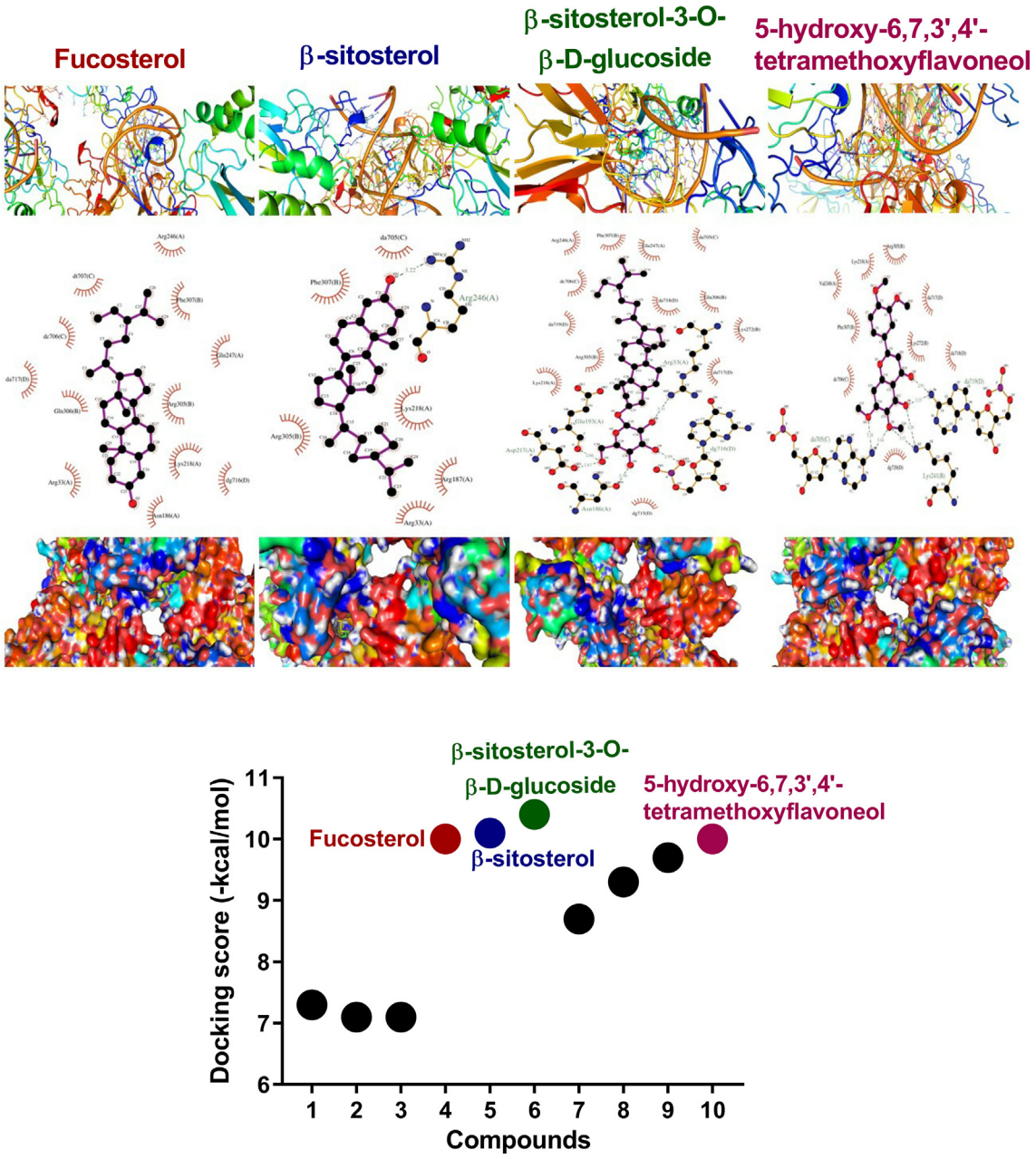

Fig. 7. Molecular docking models of the compounds **4**, **5**, **6** and **10** isolated from PEFCS with NF-κB and docking score of all compounds.

analysis of PEFCS showed the presence of flavonoids, sterols and coumarins where isoscopoletin, aesculetin, altechromone A, fucosterol, *β*-sitosterol, *β*-sitosterol-3-O-*β*-D-glucoside, scopolin, 5,7,2′-trihydroxyflavone, 5,7,2′-trihydroxy-6-methoxyflavone and 5-hyd roxy-6,7,3′,4′-tetramethoxyflavone have been identified.

The *in vivo* results revealed that rats received CIS exhibited hepatocyte injury marked by elevated transaminases and ALP which represent a sensitive marker of liver injury and hepatocyte damage. CIS-induced liver injury was supported by the microscopic findings, adding support to previous investigations revealing elevated transaminases and hepatocyte injury following the administration of CIS (Sami et al., 2023). PEFCS ameliorated liver function marker and tissue injury in CIS-treated rats. In support of our findings, *C. salicornicum* has shown a protective activity against carbon tetrachloride hepatotoxicity where it ameliorated serum transaminases and prevented tissue injury (Ahmad and Eram 2011).

Oxidative stress is a central mechanism in CIS hepatotoxicity (Sami et al., 2023) and the current study supported this role by reporting elevation of ROS, MDA, and NO along with diminished antioxidants. The cytotoxic mechanism of CIS includes the increase in ROS formation that can promote LPO, sulfhydryl depletion, signal transduction alterations and DNA damage, resulting in cell death (Florea and Büsselberg 2011). ROS can also provoke mitochondrial dysfunction through altering its respiratory function, permeability transition and Ca^{2+} homeostasis, events that with the assist of Bax promote mitochondrial DNA damage and mitochondrial damage (Green 1998). LPO negatively impacts the membrane permeability and elicits membrane damage, and increased

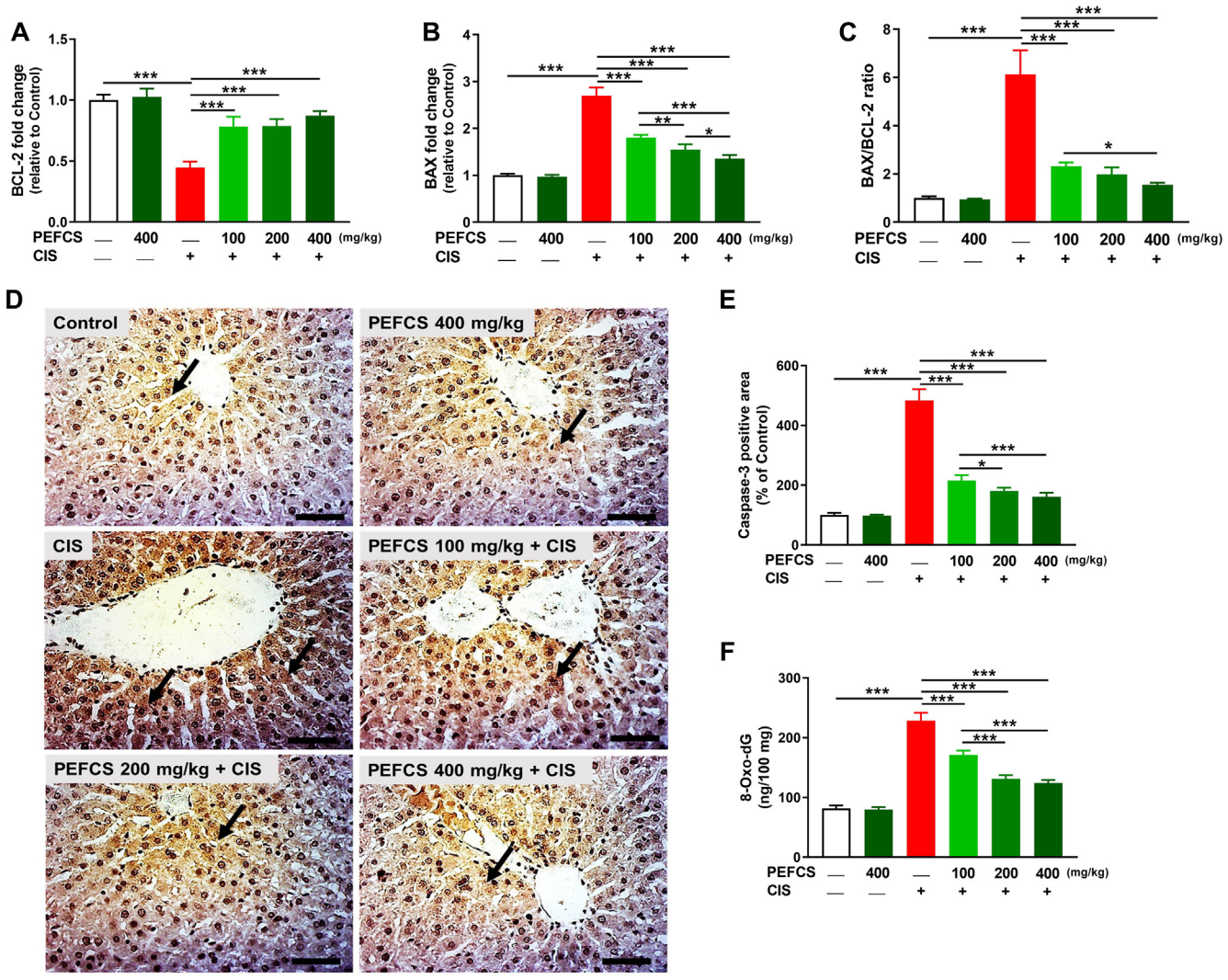

Fig. 8. PEFCS prevented apoptosis and DNA damage in liver of CIS-administered rats. PEFCS increased BCL-2 mRNA abundance (A), and decreased BAX mRNA (B) and BAX/BCL-2 ratio (C). Photomicrographs of caspase-3-immunostained sections in the liver of rats (D) and image analysis showing ameliorated expression of caspase-3 in CIS-treated rats treated with PEFCS (E). PEFCS decreased hepatic 8-Oxo-dG in changes in CIS-treated rats (F). Data are Mean ± SEM, (n = 6). *P < 0.05, **P < 0.01 and ***P < 0.001.

NO can generate peroxynitrite, resulting in DNA damage (McKim et al., 2003).

Besides redox imbalance, inflammation evidenced by upregulated inflammatory mediators was observed in CIS-treated rats. Increased ROS by CIS activates NF-κB and subsequent release of pro-inflammatory cytokines and activation of iNOS (Auten and Davis 2009), a finding that explained the reported increase in NO in this study. Peroxynitrite is another activator of NF-κB and the release of pro-inflammatory cytokines from Kupffer cells (KCs). ROS and cytokines orchestrate cell injury via apoptosis mediated through the deterioration of mitochondrial membrane potential (MMP) and activation of Bax (Shi et al., 2003). ROS and Bax deteriorate MMP resulting in the outflow of cytochrome *c* which activates caspase-3. Activated caspase-3 cleaves key structural and cell cycle proteins, and DNA followed by blebbing and condensing of cells and ultimately death of the cells (Thomsen et al., 2013). Here, Bcl-2 was declined whereas Bax, caspase-3 and 8-Oxo-dG were increased in CIS-treated rats.

PEFCS mitigated ROS, LPO and NF-κB activation and suppressed NO, iNOS, TNF-α and IL-1β in CIS-administered rats. In addition, PEFCS increased GSH, SOD, CAT, and Bcl-2 and downregulated Bax, caspase-3 and 8-Oxo-dG in the liver of rats treated with CIS. A beneficial role of PEFCS was found against oxidative and inflammatory responses and their associated cell death. The effects of PEFCS could be explained by its rich content of active constituents. Our investigation revealed the presence of coumarins, sterols and flavonoids, compounds with established hepatoprotective and radical-scavenging properties (Mahmoud et al., 2017b; Sayed et al., 2020). For instance, aesculetin attenuated inflammation by inhibiting NF-κB both *in vitro* and *in vivo* (Wang et al., 2022), and ameliorated oxidative stress and liver injury caused by various agents (Pandey et al., 2017, Mohamadi-Zarch et al., 2021). Fucosterol showed antioxidant properties and prevented NF-κB activation and acute liver injury in mice (Mo et al., 2018). Scopolin prevented liver steatosis (Yoo et al., 2017) and effectively prevented inflammation in arthritis (Pan et al., 2009), and β-sitosterol can modulate oxidative stress, NO and inflammatory cytokines (Kaur et al., 2022). To explore the protective mechanism of PEFCS against CIS hepatotoxicity, its effect on Nrf2 signaling and microRNA-34a/SIRT1 was determined. CIS downregulated Nrf2 mRNA and HO-1 activity in the liver of rats, findings coincided with our previous studies (Mahmoud et al., 2017a–c).

PEFCS upregulated Nrf2 that increases the expression of antioxidants and suppresses ROS (Satta et al., 2017). Accordingly,

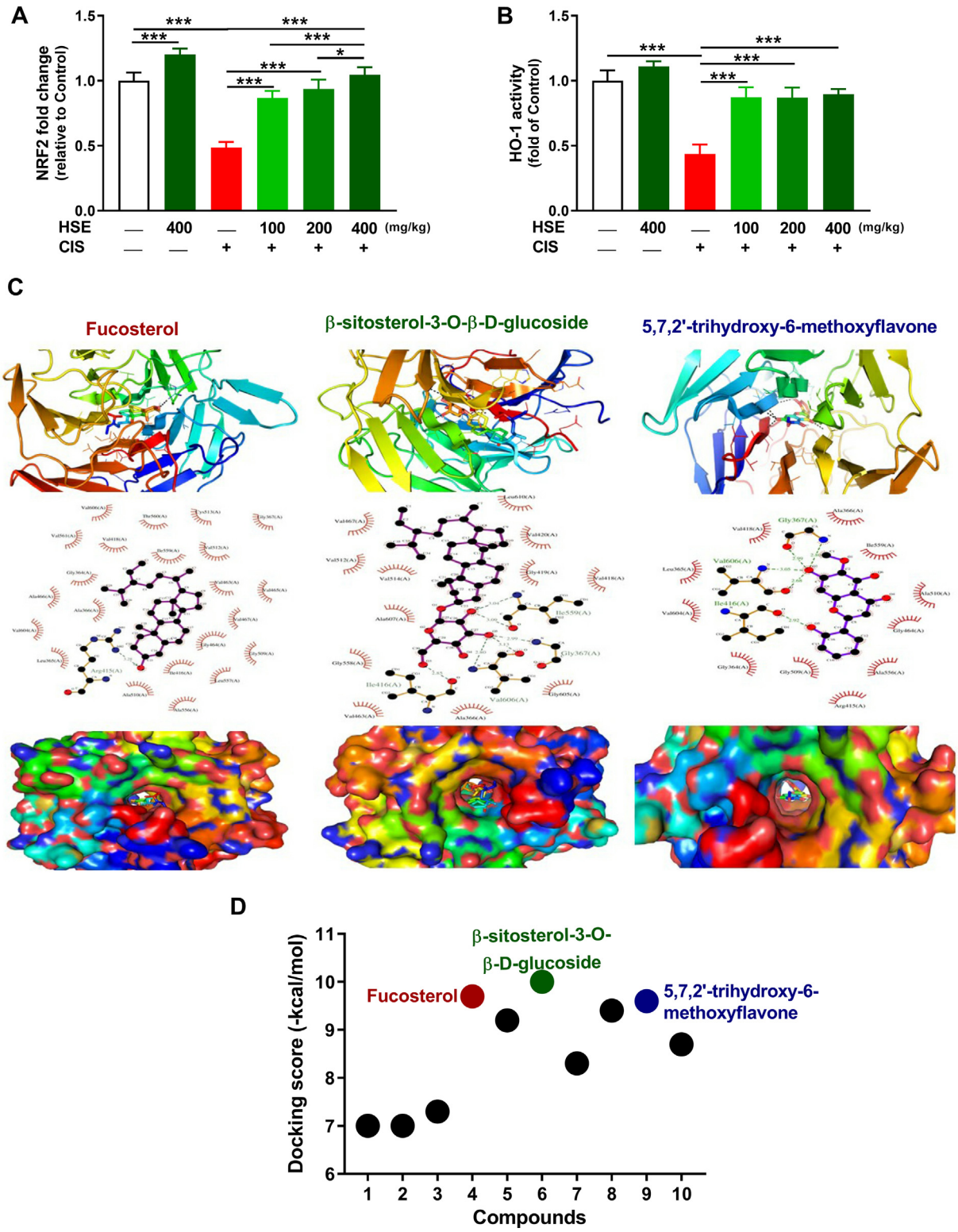

Fig. 9. PEFCS increased Nrf2 mRNA (A) and HO-1 activity (B) in the liver of CIS-administered rats. Data are Mean ± SEM, (n = 6). *P < 0.05 and ***P < 0.001. (C-D) Molecular docking models of the compounds **4**, **6** and **9** isolated from PEFCS with Keap-1 (C) and docking score of all compounds (D).

PEFCS increased HO-1 activity and this data complemented the declined ROS and the enhanced antioxidants in the liver of CIS-treated rats. HO-1 catalyzes heme degradation into biliverdin and then to the radical scavenger bilirubin (Siow et al., 1999). Activation of Nrf2 mitigated ROS, suppressed NF-κB and prevented liver injury in different animal models, whereas its depletion activated NF-κB (Pan et al., 2012). Nrf2 is an upstream regulator of the production of pro-inflammatory mediators (Kobayashi et al., 2016) and both Nrf2 and HO-1 can directly inhibit NF-κB (Wardyn et al., 2015). Therefore, upregulation of Nrf2 signaling by PEFCS resulted in attenuation of liver injury in CIS-induced rats, possibly through redox-dependent and independent mechanisms. SIRT1 activation and the downregulation of its repressor microRNA-34a participated, at least in part, to

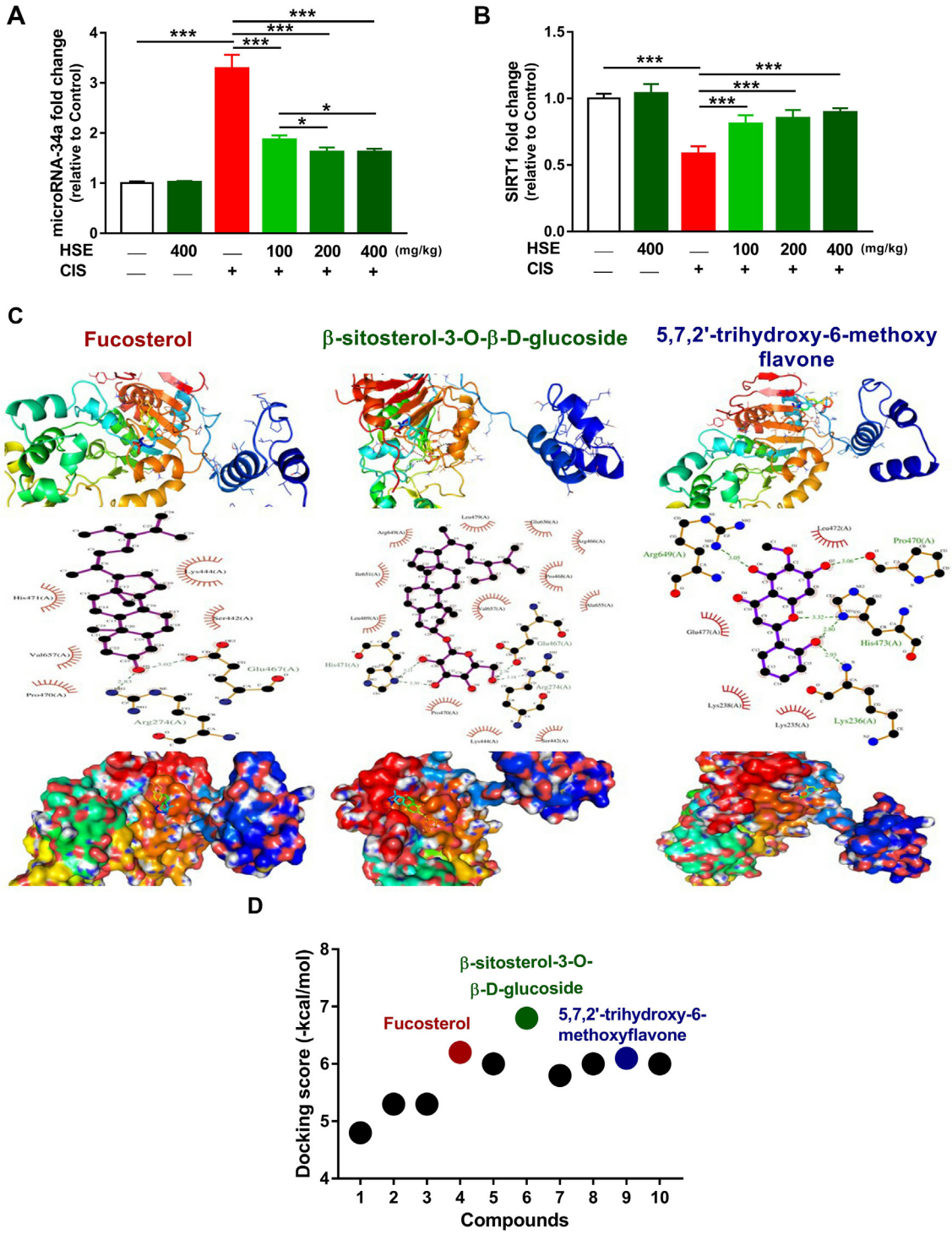

Fig. 10. PEFCS downregulated microRNA-34a (A) and increased SIRT1 mRNA abundance (B) in the liver of CIS-administered rats. Data are Mean ± SEM, (n = 6). *P < 0.05 and ***P < 0.001. (C-D) Molecular docking models of the compounds **4**, **6** and **9** isolated from PEFCS with SIRT1 (C) and docking score of all compounds (D).

the hepatoprotective activity of PEFCS. Oxidative stress has been reported to activate microRNA-34a via PI3Kα leading to reduced expression of SIRT1 (Baker et al., 2016). Therefore, suppression of ROS by PEFCS could explain the ameliorated microRNA-34a and SIRT1expression. SIRT1 improved mitochondrial function and redox balance and confers cell protection by deacetylating key metabolic players (Guarente 2013). It deacetylates PPARγ coactivator 1 alpha that promotes SOD and CAT (Olmos et al., 2013), Lys310 of the p65 subunit and therefore negatively regulates NF-κB activity (Chen et al., 2020), and p53 resulting in inhibiting its oxidative stress-induced apoptotic activity (Vaziri et al., 2001).

Molecular docking simulations were employed to investigate the modulatory effect of PEFCS on NF-κB, Nrf2 and SIRT1. Estimating polar and hydrophobic interactions of drugs with residues in the active site of the protein is a crucial tool in studying the stabilities and compatibilities of these macromolecular complexes. Particularly, hydrogen bonding is believed to be responsible for the binding of drugs into the active site of the protein, and consequently these polar interactions can compete successfully in the

molecular recognition and orientation mechanisms. A second major factor contributing to the stability of these complexes is the binding energy. Polar interactions can contribute to these binding affinities based on the number of formed hydrogen bonds and the desolvation energy. Thus, for a thermodynamically favorable drug-protein interaction, it is essential for the drug to exhibit the most suitable geometrical alignment with the protein's active site. Obviously, the coincidence of MD and the biochemical findings indicated that the elevated affinities between Keap1, NF-κB and SIRT1 and the isolated phytochemicals may mediate their antioxidant and inflammatory activities.

Catalyzed biotransformation processes proceeding by the deactivations of NF-κB could occur by preventing of one or more protein subunits, resulting in the restriction of DNA binding activity. While indirect mechanisms comprise inhibitors that modulate the NF-κB mechanism of action resulting in minimizing DNA binding activity. This study revealed the ability of *H. salicornicum* phytochemicals to modulate NF-κB. Furthermore, widely recognized substantial core residues were detected with almost all isolated phytochemicals. These residues exhibit strong electrostatic interaction with DNA during NF-κB based gene expression (Gobec et al., 2015). Consequently, blocking the binding with DNA is one of the potential mechanisms by which isolated compounds inhibited NF-κB activation (Švajger et al., 2012).

The isolated phytochemicals occupied nearly the same binding pocket of Keap1 with variable number of interacting residues depending on the structural variations. Compounds **4** and **6** exhibited the largest number of hydrophobic interactions and consequently they showed the lowest binding energy, confirming the potency of these compounds against Keap1. Hydrogen bonds were detected between oxo moieties of the phytochemicals and active site residues. The strong coexistence of polar and hydrophobic interactions revealed the stability and compatibility of isolated compounds to Keap1 binding pocket leading to mediating Nrf2 activation (Liu et al., 2017). Therefore, the conceivable influential function of isolated compounds is to interact with Keap1 and suppress its binding with Nrf2 resulting in promoting the transcriptional expression of Nrf2-targeting antioxidant genes. The obtained binding affinities of isolated compounds with SIRT1 revealed their powerful binding ability with the surface of the protein. Besides the hydrophobic interactions, three to four hydrogen bonds were detected for all compounds with SIRT1 at key residues in these drug-protein interactions.

5. Conclusion

C. salicornicum is rich in beneficial phytochemicals and our findings introduced novel information and its extract prevented CIS hepatotoxicity. PEFCS prevented hepatocyte injury, oxidative damage, inflammatory response, and apoptosis induced by CIS in dose-dependent manner. It suppressed ROS, NF-κB p65, pro-inflammatory mediators, oxidative DNA damage, pro-apoptotic factors and miR-34a. In addition, PEFCS boosted antioxidants and upregulated, SIRT1, and Nrf2/HO-1 signaling. The binding affinities between *C. salicornicum* phytochemicals and Keap1, SIRT1, and NF-κB were shown *in silico*. Therefore, PEFCS may represent a promising candidate against hepatotoxicity and could be an adjuvant therapy in patients on CIS-based chemotherapy, pending further studies to assess its exact mechanism(s) of action.

Declaration of Competing Interest

The authors declare that they have no known competing financial interests or personal relationships that could have appeared to influence the work reported in this paper.

Acknowledgment

Princess Nourah bint Abdulrahman University Researchers Supporting Project Number (PNURSP2023R381), Princess Nourah bint Abdulrahman University, Riyadh, Saudi Arabia.

Appendix A. Supplementary material

Supplementary data to this article can be found online at https://doi.org/10.1016/j.jsps.2023.101766.

References

Abraham, N.G., Lutton, J.D., Levere, R.D., 1985. Heme metabolism and erythropoiesis in abnormal iron states: role of delta-aminolevulinic acid synthase and heme oxygenase. Exp. Hematol. 13, 838–843.
Agrawal, P.K., 2013. Carbon-13 NMR of flavonoids. Elsevier.
Ahmad, M., Eram, S., 2011. Hepatoprotective studies on Haloxylon Salicornicum: a plant from Cholistan desert. Pak. J. Pharm. Sci. 24, 377–382.
Aithal, G.P., 2015. Pharmacogenetic testing in idiosyncratic drug-induced liver injury: current role in clinical practice. Liver Int. 35, 1801–1808.
Ajabnoor, M., Al-Yahya, M., Tariq, M., et al., 1984. Antidiabetic activity of Hammada salicornica. Fitoterapia 55, 107–109.
Alwahsh, M.A.A., Khairuddean, M., Chong, W.K., 2015. Chemical constituents and antioxidant activity of Teucrium barbeyanum Aschers. Rec. Nat. Prod. 9, 159–163.
Auten, R.L., Davis, J.M., 2009. Oxygen toxicity and reactive oxygen species: The devil is in the details. Pediatr. Res. 66, 121–127.
Azizuddin, A.M.K., Mustafa, S., 2013. An update on secondary metabolites from Haloxylon species. J. Chem. Soc. Pak. 35, 1551–1572.
Baker, J.R., Vuppusetty, C., Colley, T., et al., 2016. Oxidative stress dependent microRNA-34a activation via PI3Kα reduces the expression of sirtuin-1 and sirtuin-6 in epithelial cells. Sci. Rep. 6, 35871.
Bao, W., Wang, Q., Hao, J., 2019. Structural Elucidation of a Coumarin with New Skeleton from Artemisia ordosica. Rec. Nat. Prod. 13, 413–417.
Bernal, W., Wendon, J., 2013. Acute liver failure. N. Engl. J. Med. 369, 2525–2534.
Bibi, N., Tanoli, S.A., Farheen, S., et al., 2010. In vitro antituberculosis activities of the constituents isolated from Haloxylon salicornicum. Bioorg. Med. Chem. Lett. 20 (14), 4173–4176.
Bleibel, W., Kim, S., D'Silva, K., et al., 2007. Drug-induced liver injury: review article. Dig. Dis. Sci. 52, 2463–2471.
Boulos, L., 2005. Flora of egypt, Al Hadara Publishing Cairo.
Brozovic, A., Ambriović-Ristov, A., Osmak, M., 2010. The relationship between cisplatin-induced reactive oxygen species, glutathione, and BCL-2 and resistance to cisplatin. Crit. Rev. Toxicol. 40, 347–359.
Chen, Q., Ma, J., Yang, X., et al., 2020. SIRT1 mediates effects of FGF21 to ameliorate cisplatin-induced acute kidney injury. Front. Pharmacol. 11, 241.
Cohen, G., Dembiec, D., Marcus, J., 1970. Measurement of catalase activity in tissue extracts. Anal. Biochem. 34, 30–38.
Ellman, G.L., 1959. Tissue sulfhydryl groups. Arch. Biochem. Biophys. 82, 70–77.
Falsone, G., Cateni, F., Vrech, E., 1994. Triacylglycerols, fucosterol, diacylglyceroglycolipids and fucoxanthin from Fucus virsoides. J. Ag. Z. Nat. 49, 1297–1304.
Florea, A.M., Büsselberg, D., 2011. Cisplatin as an anti-tumor drug: cellular mechanisms of activity, drug resistance and induced side effects. Cancers 3, 1351–1371.
Ghosh, S., 2019. Cisplatin: The first metal based anticancer drug. Bioorg. Chem. 88, 102925.
Gobec, M., Tomašič, T., Markovič, T., et al., 2015. Antioxidant and anti-inflammatory properties of 1, 2, 4-oxadiazole analogs of resveratrol. Chem. Biol. Interact. 240, 200–207.
Green, D.R., 1998. Apoptotic pathways: the roads to ruin. Cell 94, 695–698.
Grisham, M.B., Johnson, G.G., Lancaster Jr., J.R., 1996. Quantitation of nitrate and nitrite in extracellular fluids. Methods Enzymol. 268, 237–246.
Guarente, L., 2013. Calorie restriction and sirtuins revisited. Genes Dev. 27, 2072–2085.
Haigis, M.C., Guarente, L.P., 2006. Mammalian sirtuins–emerging roles in physiology, aging, and calorie restriction. Genes Dev. 20, 2913–2921.
Kaur, K., Singh, L., Kaur, A., et al., 2022. Exploring the possible mechanism involved in the anti-nociceptive effect of β-sitosterol: modulation of oxidative stress, nitric oxide and IL-6. Inflammopharmacology 31 (1), 517–527.
Kobayashi, E.H., Suzuki, T., Funayama, R., et al., 2016. Nrf2 suppresses macrophage inflammatory response by blocking proinflammatory cytokine transcription. Nat Commun 7, 11624.
Li, L., L.-W. Xu, Y.-F. Jiang, et al., 2004. Isolation, characterization and crystal structure of natural eremophilenolide from Ligularia sagitta. Z. Naturforsch. 59b, 921–924.
Liu, Q., Hu, Y., Cao, Y., et al., 2017. Chicoric acid ameliorates lipopolysaccharide-induced oxidative stress via promoting the Keap1/Nrf2 transcriptional signaling pathway in BV-2 microglial cells and mouse brain. J. Agric. Food Chem. 65, 338–347.

Livak, K.J., Schmittgen, T.D., 2001. Analysis of relative gene expression data using real-time quantitative PCR and the 2(-Delta Delta C(T)) Method. Methods 25 (4), 402–408.
Mahmoud, A.M., Germoush, M.O., Alotaibi, M.F., et al., 2017a. Possible involvement of Nrf2 and PPARgamma up-regulation in the protective effect of umbelliferone against cyclophosphamide-induced hepatotoxicity. Biomed Pharmacother 86, 297–306.
Mahmoud, A.M., Hussein, O.E., Hozayen, W.G., et al., 2017b. Methotrexate hepatotoxicity is associated with oxidative stress, and down-regulation of PPARgamma and Nrf2: Protective effect of 18beta-Glycyrrhetinic acid. Chem. Biol. Interact. 270, 59–72.
Mahmoud, A.M., Mohammed, H.M., Khadrawy, S.M., et al., 2017c. Hesperidin protects against chemically induced hepatocarcinogenesis via modulation of Nrf2/ARE/HO-1, PPARgamma and TGF-beta1/Smad3 signaling, and amelioration of oxidative stress and inflammation. Chem. Biol. Interact. 277, 146–158.
Marklund, S., Marklund, G., 1974. Involvement of the superoxide anion radical in the autoxidation of pyrogallol and a convenient assay for superoxide dismutase. Eur. J. Biochem. 47, 469–474.
McKim, S.E., Gäbele, E., Isayama, F., et al., 2003. Inducible nitric oxide synthase is required in alcohol-induced liver injury: studies with knockout mice. Gastroenterology 125, 1834–1844.
Miyaichi, Y., Hanamitsu, E., Kizu, H., et al., 2006. Studies on the Constituents of Scutellaria Species (XXII). Constituents of the Roots of Scutellaria amabilis H ARA.Chem. Pharm, Bull, (Tokyo) 54 (4), 435–441.
Mo, W., Wang, C., Li, J., et al., 2018. Fucosterol protects against Concanavalin A-induced acute liver injury: Focus on P38 MAPK/NF-κB pathway activity. Gastroenterol. Res. Pract. 2018, 2824139.
Mohamadi-Zarch, S.M., Baluchnejadmojarad, T., Nourabadi, D., et al., 2021. Esculetin alleviates acute liver failure following lipopolysaccharide/D-galactosamine in male C57BL/6 mice. Iran J. Med. Sci. 46, 373–382.
Moore, T.J., Cohen, M.R., Furberg, C.D., 2007. Serious adverse drug events reported to the Food and Drug Administration, 1998–2005. Arch. Intern. Med. 167, 1752–1759.
Nes, W.D., Norton, R.A., Benson, M., 1992. Carbon-13 NMR studies on sitosterol biosynthesized from [13C] mevalonates. Phytochemistry 31, 805–811.
Ohkawa, H., Ohishi, N., Yagi, K., 1979. Assay for lipid peroxides in animal tissues by thiobarbituric acid reaction. Anal. Biochem. 95, 351–358.
Olmos, Y., Sanchez-Gomez, F.J., Wild, B., et al., 2013. SirT1 regulation of antioxidant genes is dependent on the formation of a FoxO3a/PGC-1alpha complex. Antioxid. Redox Signal. 19, 1507–1521.
Pan, R., Dai, Y., Gao, X., et al., 2009. Scopolin isolated from Erycibe obtusifolia Benth stems suppresses adjuvant-induced rat arthritis by inhibiting inflammation and angiogenesis. Int. Immunopharmacol. 9, 859–869.
Pan, H., Wang, H., Wang, X., et al., 2012. The absence of Nrf2 enhances NF-kappaB-dependent inflammation following scratch injury in mouse primary cultured astrocytes. Mediators Inflamm. 2012, 217580.
Pandey, A., Raj, P., Goru, S.K., et al., 2017. Esculetin ameliorates hepatic fibrosis in high fat diet induced non-alcoholic fatty liver disease by regulation of FoxO1 mediated pathway. Pharmacol. Rep. 69, 666–672.
Raynes, R., Brunquell, J., Westerheide, S.D., 2013. Stress inducibility of SIRT1 and its role in cytoprotection and cancer. Genes Cancer 4, 172–182.
Rehman, N.U., Hussain, H., Al-Riyami, S.A., et al., 2018. Chemical constituents isolated from Lycium shawii and their chemotaxonomic significance.Rec. Nat. Prod. 12, 380–384.
Russmann, S., Kullak-Ublick, G.A., Grattagliano, I., 2009. Current concepts of mechanisms in drug-induced hepatotoxicity. Curr. Med. Chem. 16, 3041–3053.
Sami, D.H., Soliman, A.S., Khowailed, A.A., et al., 2022. 7-hydroxycoumarin modulates Nrf2/HO-1 and microRNA-34a/SIRT1 signaling and prevents cisplatin-induced oxidative stress, inflammation, and kidney injury in rats. Life Sci. 310, 121104.
Sami, D.H., Soliman, A.S., Khowailed, A.A., et al., 2023. The protective effect of 7-hydroxycoumarin against cisplatin-induced liver injury is mediated via attenuation of oxidative stress and inflammation and upregulation of Nrf2/HO-1 pathwa. Environ. Sci. Pollut. Res. 30, 80181–80191.
Satta, S., Mahmoud, A.M., Wilkinson, F.L., et al., 2017. The role of Nrf2 in cardiovascular function and disease. Oxid. Med. Cell. Longev. 2017, 9237263.
Sayed, A.M., Hassanein, E.H.M., Salem, S.H., et al., 2020. Flavonoids-mediated SIRT1 signaling activation in hepatic disorders. Life Sci. 259, 118173.
Shi, Y., Chen, J., Weng, C., et al., 2003. Identification of the protein-protein contact site and interaction mode of human VDAC1 with Bcl-2 family proteins. Biochem. Biophys. Res. Commun. 305, 989–996.
Siow, R.C., Sato, H., Mann, G.E., 1999. Heme oxygenase-carbon monoxide signalling pathway in atherosclerosis: anti-atherogenic actions of bilirubin and carbon monoxide? Cardiovasc Res 41 (2), 385–394.
Švajger, U. and M. J. I. r. o. i. Jeras, 2012. Anti-inflammatory effects of resveratrol and its potential use in therapy of immune-mediated diseases. Int. Rev. Immunol. 31, 202-222.
Thomsen, N.D., Koerber, J.T., Wells, J.A., 2013. Structural snapshots reveal distinct mechanisms of procaspase-3 and-7 activation. Proc. Natl. Acad. Sci. USA 110, 8477–8482.
Tsukamoto, H., Hisada, S., Nishibe, S.J.C., et al., 1985. Coumarin and secoiridoid glucosides from bark of Olea africana and Olea capensis. Chem. Pharm. Bull. 33 (1), 396–399.
Vaziri, H., Dessain, S.K., Ng Eaton, E., et al., 2001. hSIR2(SIRT1) functions as an NAD-dependent p53 deacetylase. Cell 107, 149–159.
Wang, S.K., Chen, T.X., Wang, W., et al., 2022. Aesculetin exhibited anti-inflammatory activities through inhibiting NF-κB and MAPKs pathway in vitro and in vivo. J. Ethnopharmacol. 296, 115489.
Wardyn, J.D., Ponsford, A.H., Sanderson, C.M., 2015. Dissecting molecular cross-talk between Nrf2 and NF-κB response pathways. Biochem. Soc. Trans. 43, 621–626.
Yoo, A., Narayan, V.P., Hong, E.Y., et al., 2017. Scopolin ameliorates high-fat diet induced hepatic steatosis in mice: potential involvement of SIRT1-mediated signaling cascades in the liver. Sci. Rep. 7, 2251.
Zhang, Y., Tao, X., Yin, L., et al., 2017. Protective effects of dioscin against cisplatin-induced nephrotoxicity via the microRNA-34a/sirtuin 1 signalling pathway. Br. J. Pharmacol. 174, 2512–2527.
Zhao, M., Chen, G., Lin, T., et al., 2020. A New Labdane Diterpene from the Aerial Parts of Chloranthus serratus. Rec. Nat. Prod. 14, 378–382.